An Economic Analysis of 5G Superfluid Networks

Luca Chiaraviglio,[1,2] Nicola Blefari-Melazzi,[1,2] Carla Fabiana Chiasserini,[2,3] Bogdan Iatco,[1]
Francesco Malandrino,[3] Stefano Salsano,[1,2]
1) EE Department, University of Rome Tor Vergata, Rome, Italy, email {name.surname}@uniroma2.it
2) Consorzio Nazionale Interuniversitario per le Telecomunicazioni, Rome, Italy
3) DET, Politecnico di Torino, Turin, Italy, email {name.surname}@polito.it

***Abstract*—We target the evaluation of a Superfluid 5G network from an economic point of view. The considered 5G architecture has notably features, such as flexibility, agility, portability and high performance, as shown by the H2020 SUPERFLUIDITY project. The proposed economic model, tailored to the Superfluid network architecture, allows to compute the CAPEX, the OPEX, the Net Present Value (NPV) and the Internal Rate of Return (IRR). Specifically, we apply our model to estimate the impact for the operator of migrating from a legacy 4G to a 5G network. Our preliminary results, obtained over two realistic case studies located in Bologna (Italy) and San Francisco (CA), show that the monthly subscription fee for the subscribers can be kept sufficiently low, i.e., typically around 5 [USD] per user, while allowing a profit for the operator.**

I. Introduction

According to different studies (see e.g. [1]), the traffic in cellular networks is going to notably increase in the forthcoming years, due to a constant rise of the number of subscribers, their mobility, and the very high bandwidth required by future applications, such as tactical Internet and high definition video services. In this context, current 4G network infrastructure may not be able to face the aforementioned challenges. To solve this issue, operators and researchers have started the investigation of new technologies, under the umbrella of 5G, which are expected to turn into reality by 2020. Such technologies include, e.g., the massive adoption of Multi User Multiple Input Multiple Output (MU-MIMO) [2], cell densification [3], softwarization of network devices [4], and the possibility to exploit commodity HardWare (HW) to run virtual resources [5].

Among the different projects focusing on 5G, SUPERFLUIDITY [6] (funded by the EU through the H2020 program) targets the design of a flexible, agile, portable and high performance 5G network architecture. The core of the project is the introduction of a *Superfluid* approach in which both services and network functions are decomposed into softwarized components, named as Reusable Functional Blocks (RFBs), which are deployed on top of physical 5G nodes. RFBs have notable features, including: i) RFBs chaining to realize more complex functionalities and provide the service required by users; ii) platform independence via softwarized functions that can be run on different HW equipments; and, iii) high performance and high flexibility, by deploying the RFBs where and when they are really needed (hence the *Superfluid* attribute of the architecture). The RFB concept is a generalization of the Virtual Network Function (VNF) concept proposed by ETSI [7]. In particular, RFBs can be arbitrarily decomposed in other RFBs, while VNFs in the ETSI model cannot be decomposed in other VNFs. Moreover, the RFBs can be mapped into different SoftWare (SW) and HW execution environments (see [6]), while the ETSI model focuses on mapping VNFs into Virtual Machines (or Containers) in traditional cloud infrastructures.[1]

In this context, several questions are arising such as: Is the 5G Superfluid network sustainable from an economic point of view? What is the cost of upgrading current 4G cells sites to support 5G services? What is the monthly subscription fee to be set in order to guarantee a net profit for the operator? The goal of this paper is to answer these questions. In particular, we derive an economic model of the Superfluid network architecture firstly proposed in [6]. We then evaluate the model over two representative scenarios. Our preliminary results, obtained over two realistic case studies, demonstrate the feasibility of the proposed solution. Specifically, we show that the architecture becomes profitable for the operator when the monthly subscription fee per user is higher or equal than 5 [USD], thus making the Superfluid solution a viable approach from an economic point of view.

Focusing on the related work, the cost modeling for an SDN/NFV based mobile 5G network is proposed in [8]. However, no indication about the subscription fee that the user should pay is provided. Moreover, the evaluation is conducted only over synthetic cases, and not realistic ones like in this work. The work in [9] details the life-cycle cost modelling for NFV/SDN based mobile networks. However, the analysis considers 4G, not 5G, networks. The total cost of ownership for a 5G network is instead investigated in [10]. However, the setup of the physical HW devices, as well as the possibility to use softwarized elements, are not considered. Finally, the closest paper to our work is [11], in which the authors have performed a preliminary evaluation of a Superfluid network under different Key Performance Indicators (KPIs) over a simple synthetic scenario. In this work, we go four steps further by introducing the following original contributions:

- defining an economic model to estimate the costs and the profits achieved by the operator;
- considering two representative case studies from realistic

[1]In this work we focus on RFBs types that can be mapped in VNFs of the ETSI model. The evaluation of other RFBs features (such as the decomposition of RFBs in smaller RFBs, and the mapping of RFBs to different software environments) will done as future work.

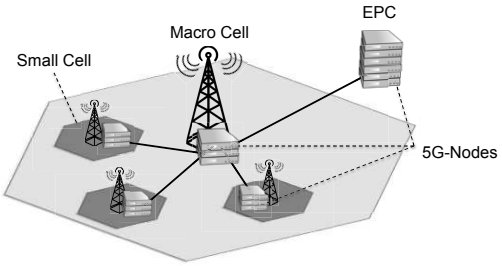

(a) Physical Infrastructure

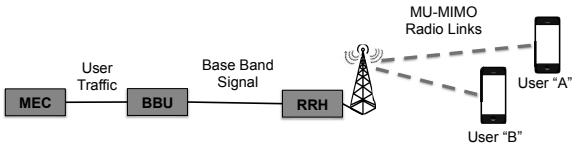

(b) RFB Connections

Fig. 1. 5G Superfluid architecture.

4G deployment, the first one located in Bologna (Italy), and the second one in San Francisco (CA);
- evaluating the impact of upgrading the existing 4G cell sites to 5G ones;
- evaluating the impact of expanding the current set of deployed cells to meet the 5G service requirements.

The rest of the paper is organized as follows. Sec. II reports the 5G Supefluid network architecture description. Sec. III details our economic model. The considered scenarios and the setting of the different components of the architecture are described in Sec. IV. Sec. V reports the results of the economic analysis over the considered scenarios. Finally, Sec. VI concludes our work.

II. 5G Superfluid Network Architecture

We briefly review the 5G Superfluid network architecture. We refer the reader to [11], [6] for a more detailed description. In brief, the 5G Superfluid network model is composed of a set of nodes, a set of links and a set of users. The nodes are used to deploy either Small Cells (SCs), Macro Cells (MCs), or to realize the core network elements of the so called Evolved Packet Core (EPC). Each node is connected to the rest of the network by means of a path of physical links. Moreover, each node is composed of Dedicated HardWare (DHW) equipment and Commodity HardWare (CHW). In addition, each user can be connected to the network by means of a cell. For simplicity, the EPC elements are collapsed into a single site in our model.

Fig. 1(a) reports an example of the considered physical system infrastructure, which is composed of different SCs, one MC and one EPC site. In this scenario, each site corresponds to a 5G node. The figure reports also the coverage areas of the cells (which are represented by hexagonal layouts for the sake of simplicity). The service area, i.e., the area where the users are located, is assumed to overlap with the coverage area of the macro cell.

In this context, the Superfluid vision aims to move from the current architectural approaches, which are based on monolithic network components/entities and their interfaces, to a solution where network functions can be programmatically composed using RFBs, which are dynamically deployed in the 5G nodes, allowing a continuous real-time optimization of the network. More in detail, the main idea behind the RFB concept is the decomposition of high-level monolithic functions into reusable components. A RFB is a logical entity that performs a set of functionalities and has a set of logical input/output ports. In addition, the RFB concept is used to model the allocation of service components to an execution platform, with the proper mapping of resources. We refer to this approach as RFB Operations. On the other hand, it is also used to explicitly model the composition of RFBs to realize a service or a component. We refer to this approach as RFB Composition. More in detail, the RFBs can be composed in graphs to provide services or to form other RFBs (therefore a RFB can be composed of other RFBs). The RFB (de)composition concept is applied to different execution environments in which the RFB can be deployed and executed. All these features make the RFB concept a generalization of the classical VNF approach, which is instead based on a rigid mapping (which can not be further decomposed) in Virtual Machines run over a traditional cloud infrastructure.

Thanks to the fact that the RFBs are fully virtualized resources, they can be dynamically moved across the nodes to satisfy the KPIs of the network operator. An RFB performs specific tasks in the network architecture, such as processing the HD video to users, or performing networking and physical layer tasks. In addition, each RFB consumes an amount of physical resources on the hosting 5G node. As physical resources we consider the *processing capacity* (that will be simply referred to as *capacity* in the rest) and the *memory occupation* (in short referred to as *memory*).

Similarly to [11], we consider the following RFBs types:

- Mobile Edge Computing (MEC) RFB;
- Base Band Unit (BBU) RFB;
- Resource Radio Head (RRH) RFB.

More in depth, each RRH RFB performs physical layer operations. In particular, the RRH module handles a set of Radio Frequency (RF) channels with users and the corresponding baseband channels with the BBU RFB. The amount of resources required by an RRH RFB depends on the type of deployed cell (denoted with "Type 1" for a MC and "Type 2" for a SC). The operations required by the RRH RFB are run on DHW equipment of the node. Focusing on the BBU RFB, this module acts as an interface between the RRH RFB and the MEC one. Specifically, the BBU RFB exchanges a baseband signal with the RRH RFB, and an amount of IP traffic with the MEC module. Its functions are run on both the DHW and CHW elements installed in the node. In our work, we assume two types of BBU RFB. Specifically, a BBU RFB of Type 1 is able to serve an RRH RFB of Type 1, while a BBU RFB of Type 2 is able to serve an RRH RFB of Type 2.

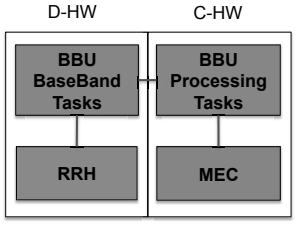

Fig. 2. RFB mapping on CHW and DHW equipment of a 5G node.

Finally, each MEC RFB is responsible for providing the HD video distribution service to the users. A practical example of a MEC RFB is a cache serving a set of videos to users.[2] In general, this module is able to serve a large amount of traffic, and consequently a subset of the users spread over the service area. The MEC functionalities are run on CHW installed in the node.

Focusing then on the interactions between the RFBs, these modules are organized in logical chains. Specifically, each MEC RFB is logically connected to a BBU RFB, which, in turn, is connected to an RRH RFB and consequently to a set of users. Fig. 1(b) reports an example of RFBs chain and the exchanged information between the modules and the users. In addition, the connection between a pair of RFBs in the chain can be direct, i.e., both RFBs are located on the same physical 5G node, or indirect, i.e., the RFBs are located on two separate nodes. In this latter case, the information flows on an external physical link. Finally, RRH RFBs are able to setup a radio link with users, by exploiting the Multi User Multiple Input Multiple Output (MU-MIMO) technology.

We now consider the placement of the RFB over the Superfluid architecture. In this context, RRH RFBs can be placed only in nodes connected to the antennas of the Radio Access Network (RAN). On the contrary, BBU RFBs can be pooled in other nodes (i.e., by exploiting the Cloud-RAN paradigm). Finally, MEC RFBs can be potentially deployed in every node of the network.

Finally, Fig. 2 reports a scheme of a 5G node, including the CHW and the DHW equipment. Specifically, the node in the example hosts one MEC RFB in the CHW, one RRH RFB in the DHW and one BBU RFB split between the CHW and DHW equipment.

III. Economic Model

In order to assess the overall profitability of the considered architecture, we need to compute the different costs and profits experienced by the operator. Specifically, the costs are divided into CAPEX and OPEX components. More in depth, the CAPEX represents the initial investment, which can be expressed as:

$$CAPEX^{TOT} = CAPEX^{MC} + CAPEX^{SC} \quad \text{[USD]} \quad (1)$$

[2]MEC functionalities are going to be implemented in current cellular networks, thus bringing notably advantages. For example, the work in [12] shows that MEC may trigger a high utilization of server resources, coupled with low latency times.

where $CAPEX^{MC}$ and $CAPEX^{SC}$ are the total CAPEX for deploying the Macro Cells (MCs) and Small Cells (SCs), respectively. $CAPEX^{MC}$ is defined as:

$$CAPEX^{MC} = N_C^{MC}\left(C^{CHW-MC} + C^{DHW-MC}\right) \quad \text{[USD]} \quad (2)$$

where N_C^{MC} is the number of MCs, C^{CHW-MC} is the commodity HW cost for an MC, and C^{DHW-MC} is the dedicated HW cost for an MC. Similarly, we define $CAPEX^{SC}$ as:

$$CAPEX^{SC} = N_C^{SC}\left(C^{CHW-SC} + C^{DHW-SC}\right) \quad \text{[USD]} \quad (3)$$

where N_C^{SC} is the number of SCs to be deployed, C^{CHW-SC} is the commodity HW cost for a SC, and C^{DHW-SC} is the dedicated HW cost for a SC.

Focusing on the OPEX, we consider the yearly electricity consumption of the cells and the yearly scheduled maintenance operations costs (which may include, e.g., HW/SW upgrades). In particular, the total electricity costs depend on the power consumption of the cells, which varies based on the current load ρ_t. In our work, we assume that the time is discretized in time slots, with a fixed duration, denoted with δ_t. The load of each cell ρ_t in each time slot varies then between a minimum and a maximum value, denoted with ρ_{min} and ρ_{max}, respectively. In addition, let us denote with P_{max}^{CHW-SC} and P_{max}^{CHW-SC} the power consumption of the CHW and DHW equipment when $\rho_t = \rho_{max}$, respectively. Similarly, let us denote with P_{min}^{CHW-SC} and P_{min}^{CHW-SC} the MC power consumption when $\rho_t = \rho_{min}$. The total yearly electricity costs C^{E-MC} of the MC at year i can be expressed as:

$$C_i^{E-MC} = \sum_t \left[\left(P_{max}^{MC} - P_{min}^{MC}\right) \cdot \left(\frac{\rho_t - \rho_{min}}{\rho_{max} - \rho_{min}}\right) + P_{min}^{MC}\right] \cdot \delta_t \cdot c \quad \text{[USD]} \quad (4)$$

where $P_{max}^{MC} = \left(P_{max}^{CHW-MC} + P_{max}^{CHW-MC}\right)$, $P_{min}^{MC} = \left(P_{min}^{CHW-MC} + P_{min}^{CHW-MC}\right)$, and c is the hourly electricity cost for one [kWh] of energy. In a similar way to Eq. 4, we define C_i^{E-SC} as the total yearly electricity costs of the SCs (not reported here due to the lack of space).

The total OPEX of the MCs for year i is then defined as:

$$OPEX_i^{MC} = N_C^{MC}(C_i^{E-MC} + C_i^{M-MC}) \quad \text{[USD]} \quad (5)$$

where C_i^{E-MC} is computed from Eq. 4, and C_i^{M-MC} is the yearly scheduled maintenance cost for a MC. In a similar way, we define the total OPEX of the SCs as:

$$OPEX_i^{SC} = N_C^{SC}(C_i^{E-SC} + C_i^{M-SC}) \quad \text{[USD]} \quad (6)$$

where C_i^{E-SC} is again computed as Eq. 4 (with the SC parameters), and C_i^{M-SC} is the yearly scheduled maintenance cost for a SC. The total OPEX for the operator is simply the sum of the previous two terms:

$$OPEX_i^{TOT} = OPEX_i^{MC} + OPEX_i^{SC} \quad \text{[USD]} \quad (7)$$

In addition, the operator earns profits from the users. Specifically, we assume that each user has to pay a monthly subscription fee, denoted with F. The total yearly profit $PROFIT_i^{TOT}$ from users is then denoted as:

$$PROFIT_i^{TOT} = N_U^{TOT} \cdot 12F \quad \text{[USD]} \quad (8)$$

We then denote the net cash flows experienced by the operator on each year as:

$$CF_i = \begin{cases} -CAPEX^{TOT} & \text{if} \quad i = 0 \\ PROFIT_i^{TOT} - OPEX_i^{TOT} & \text{if} \quad 0 < i \leq L \end{cases} \tag{9}$$

where L [years] is the lifetime of the architecture.

Given the knowledge of CF_i, a useful metric to assess the economic benefit is the Net Present Value (NPV), which is defined as:

$$NPV = \sum_{i=0}^{L} \frac{CF_i}{(1+\eta)^i} \quad \text{[USD]} \tag{10}$$

where η is the discount rate, i.e., the return (in percentage) that could be earned with a classical financial investment (such as bank funds, loans, etc.). In particular, if the NPV is larger than 0, then the operator has a monetary advantage in building the 5G architecture rather than choosing to invest the money in financial activities.

Finally, another metric to assess the deployment efficiency is the Internal Rate of Return (IRR), which is defined as the discount rate η^* making the NPV equal to 0. More formally, the IRR is the solution of the following equation:

$$\sum_{i=0}^{L} \frac{CF_i}{(1+\eta^*)^i} = 0 \tag{11}$$

Specifically, while the NPV targets the quantitative advantage of the investment, the IRR is a normalized metric, useful to compare the profitability among different deployments. Our goal will be then to assess the benefit of the proposed 5G architecture in terms of CAPEX, OPEX, NPV and IRR. To do that, we describe in the following the scenarios of practical relevance, as well as the parameters setting for the HW and RFB components.

IV. Scenarios and Components Settings

The considered scenarios are located in the cities of Bologna (Italy) and San Francisco (CA). After detailing both of them, we report the settings of the parameters for RFBs and HW components.

A. Bologna Deployment

We consider the real cell deployment of an Italian operator in the city of Bologna [13]. Tab. I reports the main features of the scenario. More in detail, the considered area A includes the entire city. In addition, we take into account the total number of users N_U^{TOT} as the sum of residents (i.e., inhabitants) and visitors (i.e., typically tourists). Focusing then on the candidate 5G cells, we consider the sites currently hosting 4G services, which will likely require the upgrade to the 5G technology in the future. Fig. 3(a) reports the real deployment of the 4G sites. Interestingly, SCs tend to concentrate in the city center where the user density is higher compared to other suburbs. However, we can note from Tab. I that the number of deployed cells N_U^{TOT} is pretty low in this scenario (i.e., dozens of cells), thus suggesting that the network may be expanded in the future in order to fully support 5G services.

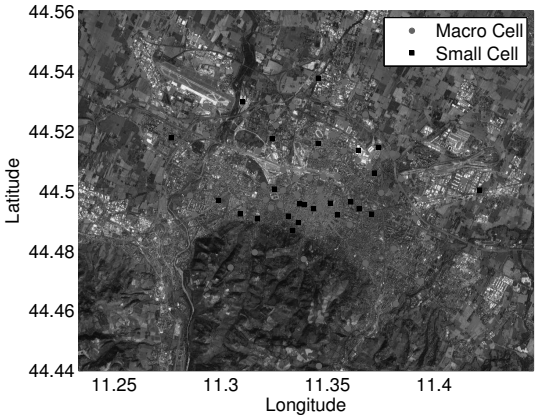

(a) Bologna Deployment

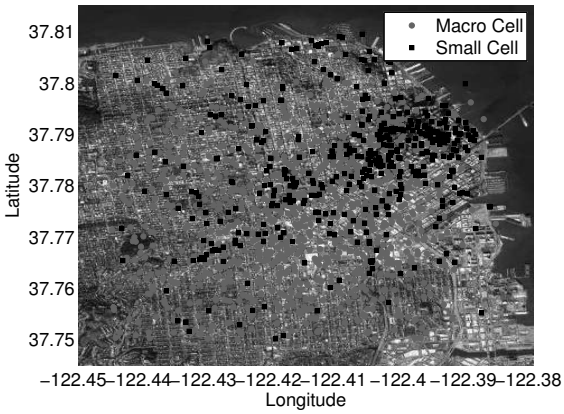

(b) San Francisco Deaployment

Fig. 3. Cellular network deployment in the two scenarios.

B. San Francisco Deployment

In the following, we consider the cell deployment of downtown San Francisco, whose main features are reported in Tab. I. In this case, the considered area A is much lower compared to the Bologna scenario. On the other hand, the user density is much higher, resulting in a total number of users comparable between the two scenarios.

As far as the cell deployment is concerned, we have adopted the methodology of [14]. Specifically, we (conservatively) assume the coverage area of each cell to be the *convex hull* of all locations from which users report being covered by the cell itself (i.e., they report the corresponding Cell ID). We then consider the radius of such a polygon, i.e., the distance between its barycenter and the farthest of its vertices. If the radius exceeds the widely accepted [15], [16] threshold of 2 km, we mark the cell as a MC; otherwise, we mark it as a SC. The position of the base station is estimated in different ways for MCs and SCs, accounting for the fact they typically use different type of antennas. In SCs, which typically employ omnidirectional antennas, we place the base station in the barycenter of the coverage area. MCs, on the other hand,

TABLE I
FEATURES OF THE CONSIDERED SCENARIOS

	Area A	Users			Cells		
		Residents	Visitors	Total (N_U^{TOT})	N_C^{MC}	N_C^{SC}	Total (N_C^{TOT})
Bologna	123 [km^2]	2413 [$1/km^2$]	19 [$1/km^2$]	299136	56	24	80
San Francisco	36 [km^2]	7124 [$1/km^2$]	600 [$1/km^2$]	278064	1027	602	1629

TABLE II
RFB PARAMETERS

RFB	Parameter	Value	
		Type 1	Type 2
RRH	Maximum Number of Users	126	42
	Maximum Served Capacity	C_{max}^{T1} =12.6 [Gbps]	C_{max}^{T2} =4.2 [Gbps]
BBU	Number of antennas generating traffic	126	42
	BBU capacity consumed on DHW	156 [Gbps]	52 [Gbps]
MEC	Maximum Served Capacity	12.6 [Gbps]	

TABLE III
CHW FEATURES

Feature	Small Cell (SC)	Macro Cell (MC)
Processor	Intel Xeon Processor E5-2630 v4, 10 Cores, 3.10 GHz.	
Memory	48 GB (1 slot 32 GB, 1 slot 16 GB)	256 GB (8 slots with 32GB)
Network Connection	Mellanox ConnectX-3 Pro Dual Port 40 GbE QSFP+ PCIE Adapter Full Height	
Power Consumption	P_{max}^{CHW-SC}=P_{max}^{CHW-MC}=450 [W] P_{min}^{CHW-SC}=P_{min}^{CHW-MC}=55 [W]	
CAPEX Cost	C^{CHW-MC}=6018 [USD]	C^{CHW-SC}=11678 [USD]

TABLE IV
DHW FEATURES

Feature	Small Cell (SC)	Macro Cell (MC)
Max. Processing Capacity	240 Gbps	640 Gbps
Power Consumption	P_{max}^{DHW-SC}=1180 [W] P_{min}^{DHW-SC}=145 [W]	P_{max}^{DHW-MC}=2180 [W] P_{min}^{DHW-MC}=269 [W]
CAPEX cost	C^{DHW-SC}=9828 [USD]	C^{DHW-MC}=29484 [USD]

usually employ directional, sectorial antennas, which we place at one of the vertices of the convex area, chosen to minimize the average distance between the base station and its served users.

Fig. 3(b) reports the obtained 4G deployment. Interestingly, in this case a very large number of 4G MCs and SCs is deployed. Similarly to the Bologna case, SCs tend to be deployed in the area with the highest user density, i.e., the one encompassing most of offices and commercial buildings.

C. RFB and HW Parameters Settings

Tab. II reports the parameter settings for RRH, BBU and MEC RFBs. We refer the reader to [11] for the detailed explanation of such settings. In brief, RRH RFBs are able to support a MU-MIMO system, assuming to serve 100 [Mbps] of average throughput to each user. In addition, BBU RFBs require a high amount of capacity, which is computed from the model of Fiorani *et. al* [17]. Moreover, the Table reports the settings for the different RFB types, i.e., Type 1 and Type 2. Specifically, an RRH RFB of Type 1 is assumed to be deployed in MC 5G nodes. RRH RFBs of Type 2 are instead installed in the 5G nodes implementing SCs. Focusing then on BBU RFB types, a BBU RFB of Type 1 can be connected only to an RRH RFB of Type 1 (the same reasoning applies also to Type 2). Finally, MEC RFBs are dimensioned to always guarantee a very high throughput per user (again assuming an average throughput of 100 [Mbps]). In this case, a single RFB type is assumed.

In the following, we focus on the main features of the CHW part of each 5G node, which are detailed in Tab. III. More in depth, the main feature impacting the total CAPEX of the CHW part is the amount of installed Random Access Memory (RAM). Clearly, an MC node has to install a large amount of RAM compared to a SC. Finally, there is not (apparently) a variation in the power consumed by the CHW part of an MC or an SC.

Tab. IV reports the main features of the DHW equipment. In this case, the processing capacity has to sustain the low-level tasks implemented by the RRH and BBU RFBs. The considered capacity values are in line with the ones retrieved from real equipment implementing MU-MIMO systems [18]. In addition, the Table provides the power consumption of the DHW part for SCs and MCs, which are taken from publicly available data [18].[3]. Finally, the Table reports the CAPEX for SCs and MCs, which are computed assuming a cost of 2340 [USD] per Gbps served to user.[4]

Finally, we consider the contributions to the OPEX. Tab. III and Tab. IV include the power consumption figures. Focusing on the load, we assume the daily variation between ρ_{min} and ρ_{max} reported by [20]. In addition, we assume $C_i^{M-MC} = C_i^{M-SC} = 2800$ [USD], i.e., the same maintenance cost for SCs and MCs. The resulting NPV and IRR are then computed assuming a total lifetime L equal to 10 years.

V. RESULTS

We initially evaluate the total CAPEX over the two scenarios, reported in Fig. 4(a). The figure shows also an upper

[3]The actual values are in line with the 5G power consumption model proposed by Fiorani *et al.* in [19].

[4]This assumption holds in the case MU-MIMO systems achieve an economy of scale, which we expect to occur in the forthcoming years.

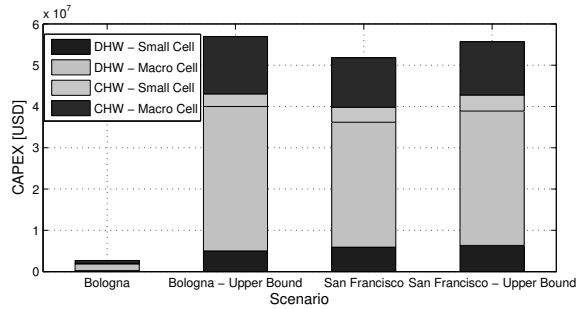

(a) Total CAPEX

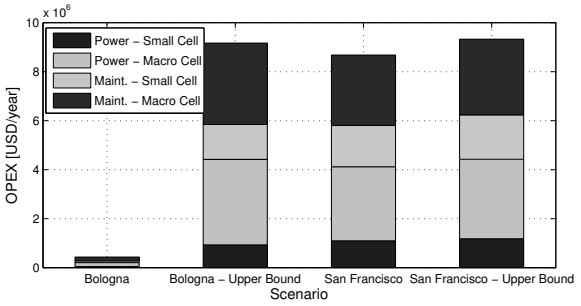

(b) Yearly OPEX

Fig. 4. Total CAPEX and yearly OPEX breakdown over the different scenarios.

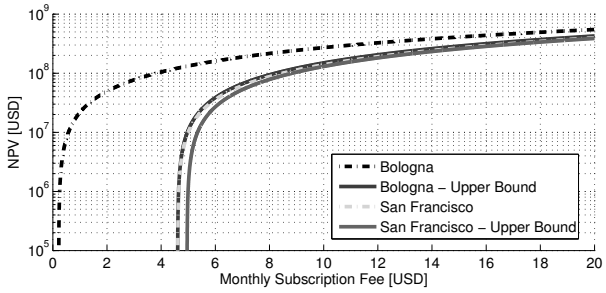

(a) NPV

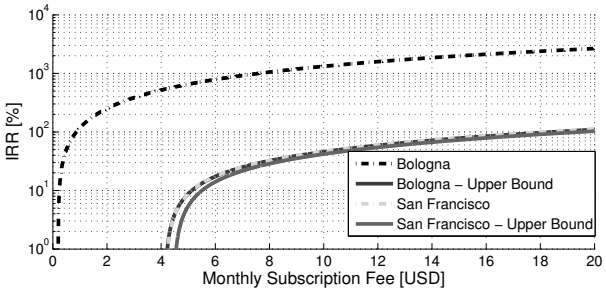

(b) IRR

Fig. 5. Net Present Value (NPV) and Internal Rate of Return (IRR) over the different scenarios.

bound, which is computed as follows. Initially, the upper bound of the number of MCs is defined as in [21]:

$$N_C^{MC-UB} = \max\left(\frac{N_U^{TOT}\cdot\alpha\cdot T}{C_{max}^{T1}}, \frac{2\cdot A}{3\sqrt{3}\cdot R_{T1}^2}\right) \quad (12)$$

where N_U^{TOT} is the total number of users (from Tab. I), α is the average user activity (assumed to be equal to 50%), T is the average traffic per user (equal to 100 [Mbps]), C_{max}^{T1} is the maximum handled capacity for an RRH RFB of type 1 (from Tab. II), A is the considered area (from Tab. I), and R_{T1} is the coverage radius of one RRH of type 1 (assumed to be equal to 3 [km]). More in detail, the model is a first-order approximation of the real behavior of the system (i.e., propagation models, power control and interference among cells are not considered). Nevertheless, we use it in order to derive general findings. In particular, the first term of Eq. 12 computes the number of MCs to guarantee the service to users, while the second term derives the number of MCs to cover the territory, assuming a simple hexagonal layout. In the following, we compute the upper bound also of the number of SCs. Specifically, SCs are used as hot spots over the territory, and not to provide coverage and capacity over the whole scenario. As a consequence, Eq. 12 can not be used in this case. To solve this issue, we define the number of SCs as:

$$N_C^{SC-UB} = \delta_C \cdot N_C^{MC-UB} \quad (13)$$

where δ_C is the ratio between MCs and SCs in the real scenario, i.e., $\delta_C = \frac{N_C^{SC}}{N_C^{MC}}$. In this way, we assume that the increase of the MCs given by the upper bound will be followed by an increase in the SCs proportional to the ratio of MCs and SCs currently deployed in the scenario. Looking back to the analysis of Fig. 4(a), we can clearly see that the costs of DHW and CHW MCs dominate over the costs of SCs. In addition, the CAPEX in the original Bologna scenario is consistently lower compared to the San Francisco one. This is due to the fact that the number of deployed cells is very low in the Bologna scenario. Specifically, when the number of deployed cells is computed by taking into account the upper bound of Eq. 12-13, the total CAPEX of the Bologna scenario becomes comparable to the San Francisco one. This suggests that the operator should perform a high investment to increase the number of deployed cells to completely fulfill the 5G requirement of providing a large amount of bandwidth to users.[5] On the other hand, the CAPEX in the San Francisco deployment is already close to its upper bound, thus suggesting that the operator should upgrade the existing sites, rather than investing a lot of money in deploying new ones.

To give more insight, Fig. 4(b) reports the yearly OPEX over the different scenarios. Similarly to the CAPEX case, the costs for MCs are higher than the ones for SCs. In addition, the electricity costs are comparable with the maintenance ones. Furthermore, we can note that, when the Bologna scenario takes into account the upper bound of the number of cells, the total OPEX is comparable to the San Francisco one. On the other hand, the OPEX in the San Francisco scenario is already close to its upper bound.

[5]Site acquisition costs for new cells are not considered in our analysis. Such costs will inevitably increase the total CAPEX incurred by the operator.

Next, we compute the NPV over our scenarios, by setting a discount rate η equal to 5%. Fig. 5(a) reports the NPV vs. the monthly subscription fee F. The vertical asymptotes in the figure are breakeven points for F generating a positive NPV, and therefore a real profit for the operator. Interestingly, the operator is able to achieve profit even when F is pretty small (i.e., around 5 [USD] per user per month). Moreover, in the original Bologna scenario, the breakeven point is even lower than 1 [USD] per month. However, in this case, the operator is not able to guarantee a user throughput of typical 5G services (such as HD video and tactile Internet). To verify this issue, we can compute the average throughput served to each user T^* from the first term of Eq. 12 (by assuming that the users are solely served by the MCs), and by considering the term N_C^{MC}, which is the number of MCs currently deployed by the operator. More formally, we can express T^* as:

$$T^* = \frac{N_C^{MC} \cdot C_{max}^{T1}}{\alpha \cdot N_U^{TOT}} \tag{14}$$

which results in $T^* = 4.72$ [Mbps] per user. Therefore, in order to fully exploit the 5G services, the number of cells should be dramatically increased in the Bologna scenario.

Finally, we consider the IRR vs. the monthly subscription fee F over the different scenarios. Fig. 5(b) reports the obtained results. In all cases, by setting $F \geq 5$ [USD] the operator is able to achieve an IRR always higher than 10%, which is the rate of typical high risk financial operations. As a result, the operator always finds it is better to invest in the upgrade of the network to provide 5G services.

VI. Conclusions and Future Works

We have proposed an economic model for a 5G Superfluid network architecture composed of SCs and MCs. We have evaluated our model over two representative case studies located in Bologna and in San Francisco. Our results, although preliminary, show that: i) the cost for deploying DHW is higher compared to CHW, ii) the monthly subscription fee for users can be kept sufficiently low, i.e., around 5 [USD] per user, while generating overall profits, iii) the Bologna network needs to be enhanced with a large number of new cell sites, in order to meet the 5G requirements.

We believe that this work can be the first step towards a more comprehensive approach. Specifically, we plan to face the design problem of a 5G network from scratch, by optimally solving the problem of deciding where to place the MCs and SCs in a given scenario. In addition, we plan to add the cost for deploying the fronthaul and the backhaul in the considered architecture. Finally, we will consider the impact of introducing smaller RFBs realizing simple functions, and the composition of these RFB together to realize more complex ones.

Acknowledgements

This work has received funding from the Horizon 2020 EU project SUPERFLUIDITY (grant agreement No. 671566).

References

[1] "Cisco Visual Networking Index: Global Mobile Data Traffic Forecast Update, 20162021 White Paper," *http://www.cisco.com/c/en/us/solutions/collateral/service-provider/visual-networking-index-vni/mobile-white-paper-c11-520862.html*.

[2] E. G. Larsson, O. Edfors, F. Tufvesson, and T. L. Marzetta, "Massive MIMO for next generation wireless systems," *IEEE Communications Magazine*, vol. 52, no. 2, pp. 186–195, 2014.

[3] N. Bhushan, J. Li, D. Malladi, R. Gilmore, D. Brenner, A. Damnjanovic, R. Sukhavasi, C. Patel, and S. Geirhofer, "Network densification: the dominant theme for wireless evolution into 5G," *IEEE Communications Magazine*, vol. 52, no. 2, pp. 82–89, 2014.

[4] R. Mijumbi, J. Serrat, J.-L. Gorricho, N. Bouten, F. De Turck, and R. Boutaba, "Network function virtualization: State-of-the-art and research challenges," *IEEE Communications Surveys & Tutorials*, vol. 18, no. 1, pp. 236–262, 2016.

[5] P. Rost, C. J. Bernardos, A. De Domenico, M. Di Girolamo, M. Lalam, A. Maeder, D. Sabella, and D. Wübben, "Cloud technologies for flexible 5G radio access networks," *IEEE Communications Magazine*, vol. 52, no. 5, pp. 68–76, 2014.

[6] G. Bianchi, E. Biton, N. Blefari-Melazzi, I. Borges, L. Chiaraviglio, P. Cruz Ramos, P. Eardley, F. Fontes, M. J. McGrath, L. Natarianni, *et al.*, "Superfluidity: a flexible functional architecture for 5G networks," *Transactions on Emerging Telecommunications Technologies*, vol. 27, no. 9, pp. 1178–1186, 2016.

[7] "ETSI GS NFV 002: Network Functions Virtualisation (NFV); Architectural Framework, V 1.2. 1," *ETSI, December*, 2014.

[8] C. Bouras, P. Ntarzanos, and A. Papazois, "Cost modeling for SDN/NFV based mobile 5G networks," in *8th International Congress on Ultra Modern Telecommunications and Control Systems and Workshops (ICUMT)*, pp. 56–61, IEEE, 2016.

[9] T. M. Knoll, "Life-cycle cost modelling for NFV/SDN based mobile networks," in *Telecommunication, Media and Internet Techno-Economics (CTTE), 2015 Conference of*, pp. 1–8, IEEE, 2015.

[10] E. J. Oughton and Z. Frias, "Exploring the Cost, Coverage and Rollout Implications of 5G in Britain," in *Cambridge: Centre for Risk Studies, Cambridge Judge Business School.*, 2016.

[11] L. Chiaraviglio, L. Amorosi, S. Cartolano, N. Blefari-Melazzi, P. Dell'Olmo, M. Shojafar, and S. Salsano, "Optimal Superfluid Management of 5G Networks," in *Proc. of 3rd IEEE Conference on Network Softwarization (IEEE NetSoft), Bologna, Italy*, July 2017.

[12] F. Malandrino, S. Kirkpatrick, and C.-F. Chiasserini, "How Close to the Edge? Delay/Utilization Trends in MEC," in *Proceedings of the 2016 ACM Workshop on Cloud-Assisted Networking*, pp. 37–42, ACM, 2016.

[13] L. Chiaraviglio, F. Cuomo, M. Maisto, A. Gigli, J. Lorincz, Y. Zhou, Z. Zhao, C. Qi, and H. Zhang, "What is the best spatial distribution to model base station density? A deep dive into two European mobile networks," *IEEE Access*, vol. 4, pp. 1434–1443, 2016.

[14] F. Malandrino, C.-F. Chiasserini, and S. Kirkpatrick, "Understanding the Present and Future of Cellular Networks through Crowdsourced Traces," in *IEEE International Symposium on a World of Wireless, Mobile and Multimedia Networks, Macao China*, ACM, June 2017.

[15] *Small Cells - Technologies and Deployment, Second and Expanded Edition*. John Wiley & Sons, 2014.

[16] S. Peric and T. Callahan, "Challenges with Microcell Deployment & Configuration," 2013. https://www.wirelessdesignmag.com/article/2013/04/challenges-microcell-deployment-configuration.

[17] M. Fiorani, B. Skubic, J. Mårtensson, L. Valcarenghi, P. Castoldi, L. Wosinska, and P. Monti, "On the design of 5G transport networks," *Photonic network communications*, vol. 30, no. 3, pp. 403–415, 2015.

[18] "BeeCube Brochure Web," *http://www.beecube.com/uploads/6/3/4/9/63495763/beecube_brochure_web.pdf*.

[19] M. Fiorani, S. Tombaz, J. Mårtensson, B. Skubic, L. Wosinska, and P. Monti, "Modeling energy performance of C-RAN with optical transport in 5G network scenarios," *Journal of Optical Communications and Networking*, vol. 8, no. 11, pp. B21–B34, 2016.

[20] G. Auer, V. Giannini, I. Gódor, P. Skillermark, M. Olsson, M. A. Imran, D. Sabella, M. J. Gonzalez, C. Desset, and O. Blume, "Cellular energy efficiency evaluation framework," in *Vehicular Technology Conference (VTC Spring), 2011 IEEE 73rd*, pp. 1–6, IEEE, 2011.

[21] M. Fiorani, S. Tombaz, P. Monti, M. Casoni, and L. Wosinska, "Green backhauling for rural areas," in *Optical Network Design and Modeling, 2014 International Conference on*, pp. 114–119, IEEE, 2014.